Proceedings of the SEM International Conference & Exposition on Experimental and Applied Mechanics June 11-12, 2012 Costa Mesa, California USA
©2012 Society for Experimental Mechanics Inc.

Improved Instrumented Indentation of Soft Materials through Surface Deformation Measurements

M.J. Wald[1*], J.M. Considine[2], K.T. Turner[1]

[1]Dept. of Mechanical Engineering and Applied Mechanics, University of Pennsylvania,
220 S. 33rd St., Philadelphia, PA 19104
[2]US Forest Service, Forest Products Laboratory,
1 Gifford Pinchot Dr., Madison, WI 53706

*mwald@seas.upenn.edu

Abstract

Instrumented indentation is a commonly used technique to determine the mechanical properties of bulk materials and thin films by measuring the load and displacement during indentation into a specimen. However, in traditional indentation measurements, it can often be difficult to determine the true deformation of the specimen due to the machine compliance and drift in the system. The issue of drift is particularly problematic in tests that occur over extended time scales, such as creep tests on soft materials. In the present work, a new method, in which the full-field deformation of the sample material around the indenter is measured, is presented to overcome these challenges. Specifically, the deformation of specimens during cylindrical flat punch indentation tests is monitored by tracking discrete particles, such as microbeads, near the surface of the sample. This method allows for direct measurement of the specimen surface as it is deformed. In the current implementation, it is applicable to transparent materials, including many polymers, gels, and biological materials. An inverse method was developed to extract mechanical properties of the specimen from the measured displacement fields. A numerical model parametric study was performed to quantify the effect of changes in Poisson's ratio, magnification, particle density, and experimental noise on the elastic properties calculated using the inverse method.

Introduction

Instrumented indentation is a common method for characterizing the mechanical properties of bulk materials. This technique is capable of testing small volumes of material at low loads and small displacements and allows for simple sample preparation compared to traditional compression tests. Oliver and Pharr [1] proposed a widely accepted method based on Sneddon's [2] solution for axisymmetric indentation of an elastic halfspace for determining a specimen's effective modulus, E_{eff}, for bulk materials from the measured applied load and displacement of the indenter. However, Young's modulus, E, and Poisson's ratio, ν, which are commonly used in engineering applications, cannot be independently measured using traditional indentation analysis. To find E, it is necessary to estimate ν, which is often difficult to measure directly for small volumes of material.

The Oliver-Pharr method is also affected by the sensitivity of measured stiffness to errors in the measurement of the true deformation of a specimen. These errors are commonly due to machine compliance and thermal drift. Machine compliance is commonly calculated by indenting a material with known elastic properties, such as fused silica, and subtracting the theoretical compliance of the material from the experimentally measured compliance [3]. While this method provides an estimate for the machine compliance, it relies on an accurate measurement of the contact area and the ability to accurately detect the specimen surface. Thermal drift, or the change in measured indenter location due to small changes in temperature, is often minimized by either conducting indentation tests in a closed environment in which the temperature is stable, or performing indentation tests quickly [4].

©2012 Society for Experimental Mechanics Inc.

In the present work, a new method is introduced in which full-field displacement of the surface of a transparent specimen, including materials such as polymers, gels, and biological materials, is measured independently of the indenter. This method tracks the motion of discrete particles, such as microbeads, near the surface of the specimen during an indentation test. The motion of particles may be tracked using optical techniques, such as fluorescence microscopy or laser confocal microscopy. Measuring full-field displacement of the specimen surface in the vicinity of the indenter allows mechanics models that relate both the in-plane displacements and out-of-plane displacements to the applied load to be used to extract elastic properties. The use of both in-plane and out-of-plane displacement permits both E and ν to be obtained. In addition, separating the displacement measurements from the indenter allows the deformation to be measured independently of machine compliance and thermal drift.

The purpose of the present work is to use numerical modeling to assess the effect of measurement error on the ability to extract elastic modulus and Poisson's ratio from experiments. A parametric study was conducted in which ν, particle density, and optical magnification, were systematically varied. For each case, 1000 simulations, with different random noise added in each, were completed. Coefficients of variation for calculated E and ν for each case were calculated and then mapped to determine combinations of particle density and magnification that are suitable for indentation experiments. The level of experimental noise applied was varied for one case to determine the effect of noise level on the coefficients of variation of E and ν.

Background

Instrumented indentation has become a popular technique for evaluating mechanical properties of soft materials, including polymers and biological tissues [5]. Cylindrical flat punch indentation was chosen because of the availability of indenters with large contact areas which are constant as a function of depth. Many soft materials of interest are porous or have a heterogeneous microstructure. Using an indenter with a contact area larger than the material's microstructure allows the average material properties to be measured. Constant contact radius with respect to indentation depth also simplifies the analysis and does not require indenter geometry to be known as a function of depth. For cylindrical flat punch indentation, as shown in Figure 1, effective modulus, which is a function of elastic modulus, E, and Poisson's ratio, ν, relates to the stiffness measured during an indentation test as follows:

$$E_{eff} = \frac{E}{1-\nu^2} = \frac{k}{2a}, \tag{1}$$

where a is the indenter contact radius, and k is the stiffness evaluated at maximum applied load.

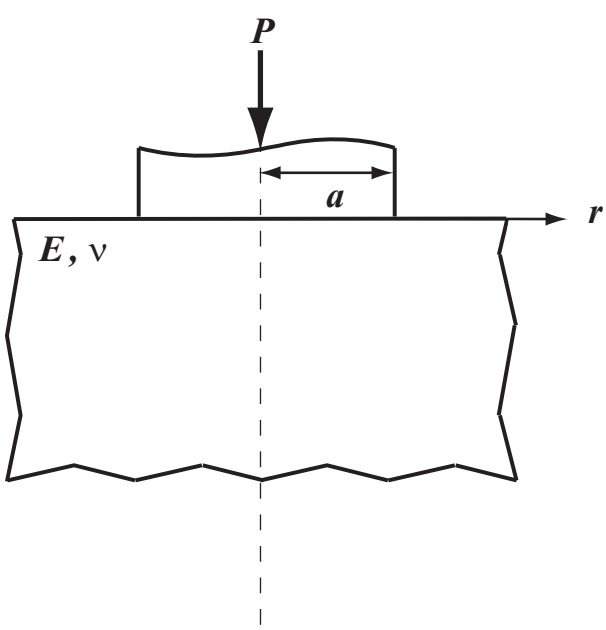

Fig. 1 Schematic of cylindrical flat punch indentation, showing applied force, P, contact radius, a, indenting an elastic halfspace with elastic modulus, E, and Poisson's ratio, ν

The in-plane and out-of-plane displacements of a point on the surface of an elastic halfspace that is being indented with a flat punch are defined as a function of E, ν, a, radial position, r, applied load, P [6]. Inside the contact area ($r<a$), the displacements are

$$u_r = -\frac{(1-2\nu)(1+\nu)}{2\pi E}\frac{P}{r}\left(1-\sqrt{1-\left(\frac{r}{a}\right)^2}\right)$$
$$u_z = \frac{1-\nu^2}{2E}\frac{P}{a}. \tag{2}$$

Outside of the contact area ($r>a$), the displacements are

$$u_r = -\frac{(1-2\nu)(1+\nu)}{2\pi E}\frac{P}{r}$$
$$u_z = \frac{1-\nu^2}{\pi E}\frac{P}{a}\arcsin\left(\frac{a}{r}\right). \tag{3}$$

©2012 Society for Experimental Mechanics Inc.

These can be rewritten in Cartesian coordinates as follows:
for $r<a$,

$$u_x = -\frac{(1-2\nu)(1+\nu)}{2\pi E}\frac{Px}{x^2+y^2}\left(1-\sqrt{1-\frac{x^2+y^2}{a^2}}\right)$$
$$u_y = -\frac{(1-2\nu)(1+\nu)}{2\pi E}\frac{Py}{x^2+y^2}\left(1-\sqrt{1-\frac{x^2+y^2}{a^2}}\right) \tag{4}$$
$$u_z = \frac{1-\nu^2}{\pi E}\frac{P}{a}$$

and for $r>a$,

$$u_x = -\frac{(1-2\nu)(1+\nu)}{2\pi E}\frac{Px}{x^2+y^2}$$
$$u_y = -\frac{(1-2\nu)(1+\nu)}{2\pi E}\frac{Py}{x^2+y^2} \tag{5}$$
$$u_z = \frac{1-\nu^2}{\pi E}\frac{P}{a}\arcsin\left(\frac{a}{\sqrt{x^2+y^2}}\right).$$

Numerical Model Methods

A simple numerical model based on equations 4 and 5 was developed to create simulated experimental displacement data with noise for a given E, ν, P, and a. This model assumes that the displacements are measured by tracking the movement of discrete particles near the surface of the specimen. The field of view represents an 8.576 mm by 6.912 mm CMOS sensor with a resolution of 1280 pixels by 1024 pixels. The field of view was aligned so one corner of the field corresponds with the center of the indenter and a quarter of the 500 μm radius indenter was in view. The dimensions of the field of view were assumed to be inversely proportional to the magnification. To simulate an experiment, Gaussian white noise with 0 mean was added to the displacement data. For in-plane displacement, the standard deviation of the noise was conservatively assumed to be 1 pixel. For out-of-plane displacement, the resolution stated for the defocused imaging technique for full-field displacement measurement reported in Wu, et al. [7] was used as an estimate of the standard deviation of the u_z noise. Similar to the dimensions of the field of view, the noise was assumed to be inversely proportional to magnification. Table 1 contains a summary of the field of view dimensions and u_x, u_y, and u_z noise.

An optimization routine was developed to extract E and ν from simulated displacement data with added noise. This routine assumed that the full field displacements near the specimen surface were measured experimentally in which the indenter radius and applied load were known. E and ν were found using a nonlinear least square algorithm, which varied E and ν to minimize error between simulated experimental data and theoretical displacements calculated from equations 4 and 5.

Table 1 Parameters for Numerical Simulations

Fixed Parameters	Parameters Varied
a = 500 μm P = 10 mN E = 2 MPa	ν = 0.1 – 0.5 magnification = 5x – 40x particle density = 100 mm^{-2} – 500 mm^{-2} u_x noise = u_y noise = 6.7 μm/magnification u_z noise = 10 μm/magnification Field of view = 8.576 mm/magnification by 6.912mm/magnification

A parametric study was conducted to investigate the effect ν, magnification, and particle density on the ability to extract E and ν from simulated displacement data. In all cases, maximum applied load was 10 mN, elastic modulus was 2 MPa, and contact radius was 500 μm. Using these parameters with a Poisson's ratio of 0.3, the maximum in-plane deflection is 0.57 μm toward the center of the indenter and occurs at a radius of 360 μm from the center of the

©2012 Society for Experimental Mechanics Inc.

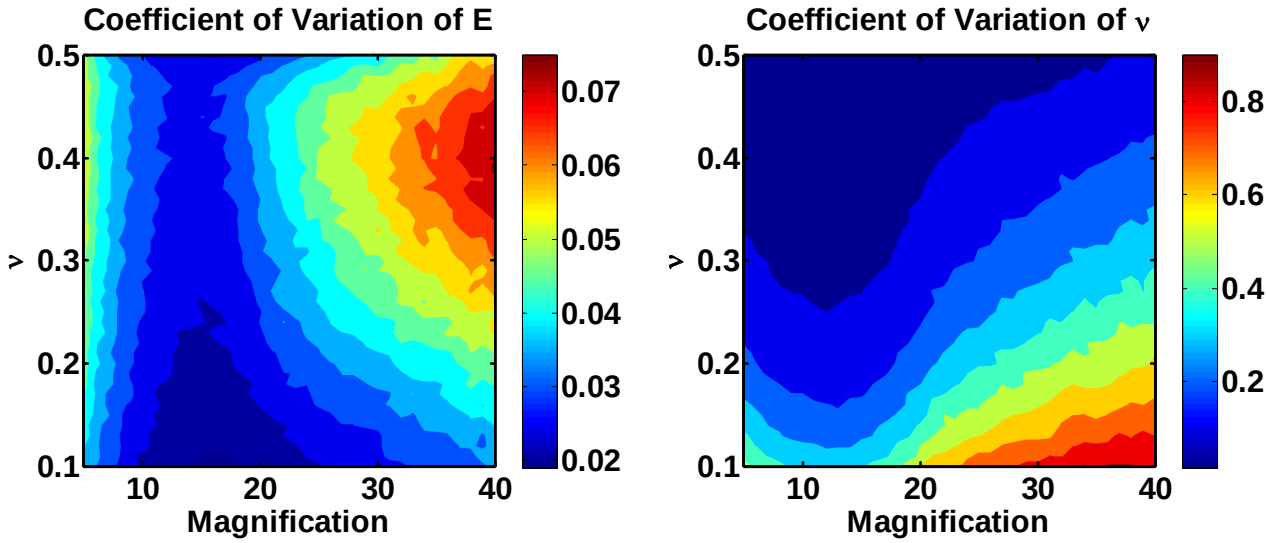

(a) (b)

Fig. 2 (a) Coefficients of variation of *E* and (b) ν as a function of ν and magnification when the particle density is 300 mm^{-2}

indenter. The maximum out-of-plane displacement is 2.90 μm and is uniform under the indenter. To account for variations in simulations due to added random noise, 1000 simulations were run for each set of parameters, allowing the effect of the parameters on the coefficients of variation of calculated elastic properties to be investigated.

Numerical Model Results

The results in this section are presented in terms of coefficient of variations. For each condition (i.e., combination of magnification, particle density, and Poisson's ratio), 1000 simulations are run and *E* and ν values are extracted for each case. The coefficient of variation values represent how much the extracted *E* and ν values vary over the 1000 simulations with different noise levels and thus are related to the probability of determining the actual *E* and ν value in a single experiment. In general, a lower coefficient of variation indicates more desirable test conditions.

Results for the numerical simulations over the range of parameters in Table 1 are summarized in Figures 2 – 4. Figure 2 shows the coefficients of variation for *E* and ν with respect to ν and the magnification with a fixed particle density of 300 mm^{-2}. Figure 2a shows that, initially, as magnification increases, the coefficient of variation decreases until it reaches a

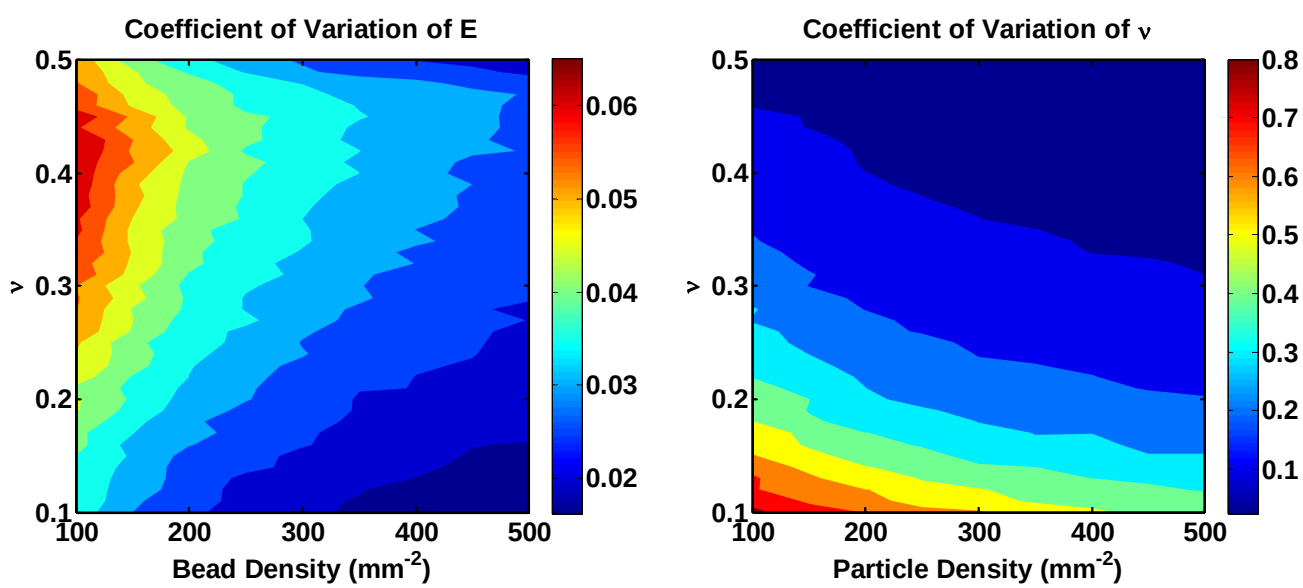

(a) (b)

Fig. 3 (a) Coefficients of variation of *E* and (b) ν as a function of ν and particle density when the magnification is 20x

©2012 Society for Experimental Mechanics Inc.

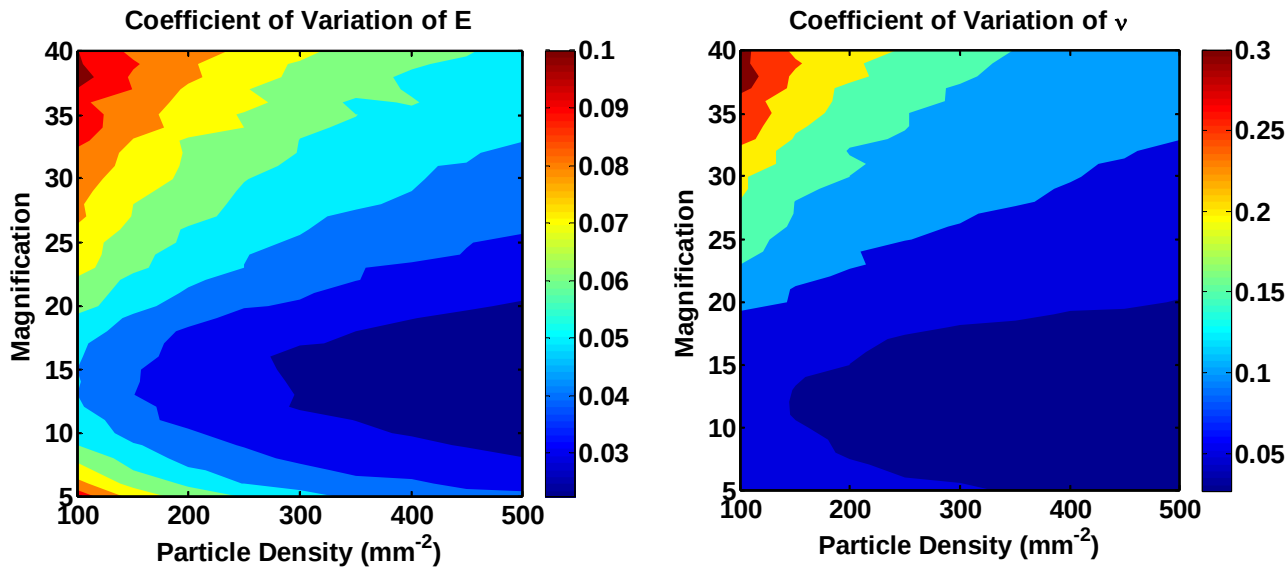

(a) (b)

Fig. 4 (a) Coefficients of variation of E and (b) ν as a function of magnification and particle density when ν is 0.45

minimum value between 10x and 20x. As magnification continues to increase, the coefficient of variation also increases. The coefficient of variation for E is largest when the magnification is 40x and ν is between 0.3 and 0.5. Similarly, Figure 2b shows that, for a given ν, the variation of ν initially decreases as magnification increases, reaching a minimum between 10x and 20x. The largest variation in ν occurs when the magnification is 40x and Poisson's ratio is 0.1. These results suggest that the pixel resolution is too coarse to measure the displacements when the magnification is below 10x. For magnifications above 20x, there may be too few particles in the field of view for accurate measurements.

Figure 3 shows the relationship between the coefficients of variation of E and ν as a function of ν and particle density when the magnification is fixed at 20x. For a constant ν, the coefficients of variation for E and ν decrease as the particle density increases. This occurs because increasing the particle density increases the number of points the algorithm uses to extract E and ν, thereby reducing the error. For the cases examined, the variation of E is largest when the particle density is 100 mm^{-2} and Poisson's ratio is about 0.4. Variation of ν (Figure 3b) is largest when the particle density is 100 mm^{-2} and Poisson's ratio is about 0.1.

The coefficients of variation of E and ν are shown as a function of magnification and bead density for a Poisson's ratio of 0.45 in Figure 4. Similar to the results shown in Figures 2 and 3, Figure 4 shows that the variation of E and ν decreases as particle density increases and the variation is smallest for magnifications between 10x and 20x. Figure 5 shows regions in which the coefficients of variation of E and ν are greater than 0.05, between 0.03 and 0.05, and less than 0.03. These results show that, for a given material, an appropriate combination of particle density and magnification can be chosen to achieve an acceptable coefficient of variation.

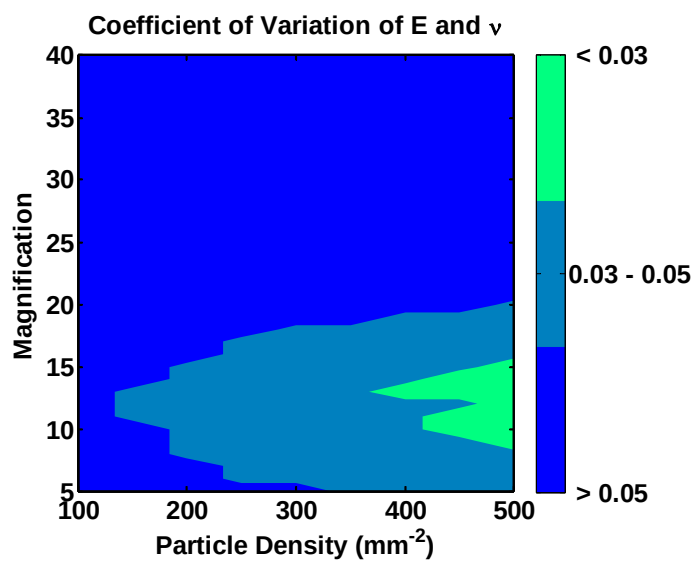

Fig. 5 Contours showing regions in which the coefficients of variation are both greater than 0.05, between 0.03 and 0.05 and less than 0.03

Because the exact noise of the proposed experiment will depend on the particular system configuration and is thus unknown, a case study was completed in which the added noise was varied. For this case study, ν was 0.45, particle density was 300 mm^{-2}, and magnification was 20x; 1000 simulations were run at each noise level. The noise was varied by proportional scaling so that the noise given in Table 1 is the maximum noise and corresponds to a noise level of 1 and no noise corresponds to a noise level of 0. As shown in Figure 6, the coefficients of variation for E

©2012 Society for Experimental Mechanics Inc.

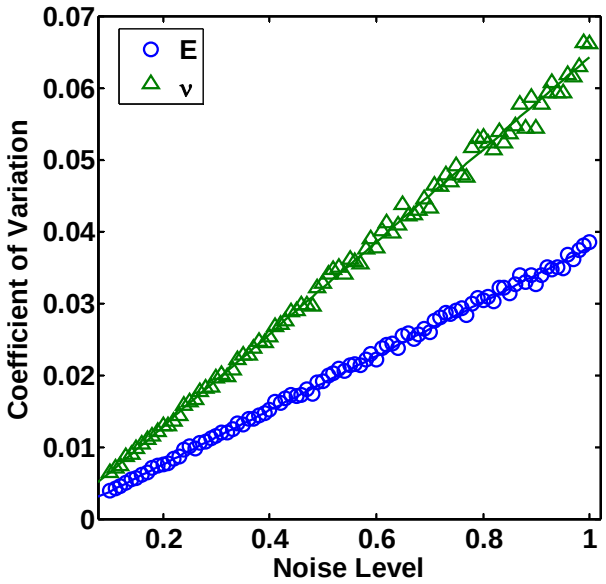

Fig. 6 Coefficients of variation of E and ν versus fraction of the maximum noise for case where ν was 0.45, magnification was 20x, and bead density was 300 mm^{-2}

and ν scale linearly with the noise level. Linear fit lines for the coefficients of variation of E and ν as a function of noise level are also shown in Figure 6. The increase in scatter as the noise level increases suggests that 1000 simulations may not be sufficient to characterize the variations as noise level increases.

The magnitudes of the displacements scale with the applied load. Since the random noise is assumed to not vary with the applied load, as the displacements increase relative to random noise, the effect of the noise on the measured results will be less significant. Conversely, when the measured displacements are smaller, noise may have a larger influence on the variation of the calculated E and ν values.

Conclusion

A numerical study was conducted to determine the effect ν, particle density and magnification have on E and ν extracted from simulated full-field displacement measurements. For the range of parameters investigated, it was determined that for a given particle density and Poisson's ratio, the coefficient of variation is smallest when the magnification is between 10x and 20x. The coefficients of variation also decrease as particle density increases. By examining the variation as a function of particle density and magnification, it was demonstrated that, for a given material, an appropriate combination of particle density and magnification can be selected to achieve an acceptable level of variation.

For a material where ν is 0.45, the bead density is 300 mm^{-2}, and the magnification is 20x, the coefficients of variation were examined as a function of noise level. Variation was shown to scale linearly with noise level. For all noise levels examined, the variation of ν was larger than the variation of E. Linear fit lines were applied to the coefficients of variation to determine the relationship of the true coefficients of variation for E and ν. As the magnitudes of the displacements scale with applied load, it may be beneficial to use larger applied loads to decrease the variation in the measurements, assuming that large loads do not alter the constitutive response. The accuracy of the proposed technique has not been considered in the current work, but it will be evaluated in the future.

Acknowledgements

We acknowledge financial support from the United States Postal Service and the US Forest Service, Forest Products Laboratory.

References

[1] Oliver, W. C. and Pharr, G. M., "An improved technique for determining hardness and elastic-modulus using load and displacement sensing indentation experiments," *Journal of Materials Research*, vol. 7, no. 6, pp. 1564-1583, 1992.

[2] Sneddon, I. N., "The relation between load and penetration in the axisymmetric Boussinesq problem for a punch of arbitrary profile," *International Journal of Engineering Science*, vol. 3, no. 1, pp. 47-57, 1965.

[3] VanLandingham, M. R., "Review of instrumented indentation," *Journal of Research of the National Institute of Standards and Technology*, vol. 108, no. 4, pp. 249-265, 2003.

[4] Nohava, J., Randall,N. X., and Conté, N., "Novel ultra nanoindentation method with extremely low thermal drift: principle and experimental results," *Journal of Materials Research*, vol. 24, no. 3, pp. 873-882, 2009.

[5] Oyen, M., "Nanoindentation of Biological and Biomimetic Materials," *Experimental Techniques*, 2011., 10.1111/j.1747-1567.2011.00716.x

©2012 Society for Experimental Mechanics Inc.

[6] Maugis, D., *Contact, Adhesion and Rupture of Elastic Solids*, 1st ed. Berlin: Springer, 2000.

[7] Wu, M., Roberts, J. W., and Buckley, M., "Three-dimensional fluorescent particle tracking at micron-scale using a single camera," *Experiments in Fluids*, vol. 38, no. 4, pp. 461-465, Feb. 2005.